

**Isotopic  
fractionation of  
stratospheric OCS**

J. A. Schmidt et al.

This discussion paper is/has been under review for the journal Atmospheric Chemistry and Physics (ACP). Please refer to the corresponding final paper in ACP if available.

# On the isotopic fingerprint exerted on carbonyl sulfide by the stratosphere

**J. A. Schmidt<sup>1</sup>, S. Hattori<sup>2</sup>, N. Yoshida<sup>2,3</sup>, S. Nanbu<sup>4</sup>, M. S. Johnson<sup>1</sup>, and R. Schinke<sup>5</sup>**

<sup>1</sup>Department of Chemistry, University of Copenhagen, Universitetsparken 5, 2100 Copenhagen Ø, Denmark

<sup>2</sup>Department of Environmental Science and Technology, Interdisciplinary Graduate School of Science and Engineering, Tokyo Institute of Technology, Yokohama, 226-8502, Japan

<sup>3</sup>Department of Environmental Chemistry and Engineering, Interdisciplinary Graduate School of Science and Engineering, Tokyo Institute of Technology, Yokohama, 226-8502, Japan

<sup>4</sup>Faculty of Science and Technology, Sophia University, 7-1 Kioi-Cho, Chiyoda-ku, Tokyo 102-8554, Japan

<sup>5</sup>Max-Planck-Institut für Dynamik und Selbstorganisation, 37073 Göttingen, Germany

Received: 10 July 2012 – Accepted: 17 September 2012 – Published: 25 September 2012

Correspondence to: J. A. Schmidt (johanalbrechtschmidt@gmail.com)

Published by Copernicus Publications on behalf of the European Geosciences Union.

Title Page

Abstract

Introduction

Conclusions

References

Tables

Figures

⏪

⏩

◀

▶

Back

Close

Full Screen / Esc

Printer-friendly Version

Interactive Discussion



## Abstract

The isotopic fractionation in OCS photolysis is studied theoretically from first principles. UV absorption cross sections for OCS, OC<sup>33</sup>S, OC<sup>34</sup>S, OC<sup>36</sup>S and O<sup>13</sup>CS are calculated using the time-depended quantum mechanical formalism and recent potential energy surfaces for the lowest four singlet and lowest four triplet electronic states. The calculated isotopic fractionations as a function of wavelength are in good agreement with recent measurements by Hattori et al. (2011) and indicate that photolysis leads to only a small enrichment of <sup>34</sup>S in the remaining pool of OCS. A simple stratospheric model is constructed taking into account the main stratospheric sink reactions of OCS and it is found that stratospheric removal overall slightly favors light OCS in contrast to the findings of Leung et al. (2002). These results show, based on isotopic considerations, that OCS is an acceptable source of background stratospheric sulfate aerosol in agreement with a recent model study of Brühl et al. (2012). The <sup>13</sup>C isotopic fractionation due to photolysis of OCS is significant and will leave a strong signal in the pool of remaining OCS making it a candidate for tracing using the ACE-FTS and MIPAS data sets.

## 1 Introduction

Carbonyl sulfide (OCS or COS) is an important trace gas and the most abundant sulfur compound in Earth's atmosphere (Montzka et al., 2007). The mixing ratio of OCS is about 500 ppt (parts-per-trillion i.e. pmolmol<sup>-1</sup>) and almost constant throughout the troposphere, and decreases rapidly with altitude in the stratosphere (Chin and Davis, 1995; Notholt et al., 2003; Barkley et al., 2008).

The sources of OCS include emission from the ocean, wetlands, soil and precipitation. The precipitation source was suggested on the basis of observations of rain water supersaturated with OCS. This source is believed to operate via chemical processes inside the rain drop (Belviso et al., 1967; Watts, 2000). Other sources of OCS

ACPD

12, 25329–25353, 2012

### Isotopic fractionation of stratospheric OCS

J. A. Schmidt et al.

Title Page

Abstract

Introduction

Conclusions

References

Tables

Figures

◀

▶

◀

▶

Back

Close

Full Screen / Esc

Printer-friendly Version

Interactive Discussion



are biomass burning, a variety of anthropogenic activities, volcanoes, and oxidation of carbon disulfide and dimethyl sulfide (Watts, 2000; Montzka et al., 2007).

The main sinks of OCS are uptake by vegetation and soils. OCS is relatively resistant to atmospheric oxidation, but the reactions with OH and ground state O are important in situ sinks. Photolysis is an important stratospheric sink of OCS (Watts, 2000).

OCS has a long atmospheric lifetime of about two years (Montzka et al., 2007; Brühl et al., 2012) which allows OCS to be transported into the stratosphere where the lifetime is longer; Chin and Davis (1995) estimated it to be about 10 yr while Barkley et al. (2008) found it to be  $64 \pm 21$  yr. The atmospheric sink reactions give products that react further and eventually form sulfur dioxide ( $\text{SO}_2$ ). OCS can therefore be a significant source of stratospheric  $\text{SO}_2$ . Crutzen (1976) suggested that the conversion of this  $\text{SO}_2$  to sulfate would in turn be a significant background source of the stratospheric sulfate aerosol (SSA) layer. This layer is important because it can enhance stratospheric ozone depletion (Solomon et al., 1993) and influence Earth's radiative balance (Turco et al., 1980; Myhre et al., 2004).

There is an ongoing debate concerning the concentration, sources and trends for the background (non-volcanic) sulfate aerosol layer. Hofmann (1990) found an increase in background SSA of 5 % per year from 1979 to 1990 at northern mid-latitudes. The background concentration of sulfate aerosol is consistently variable (Solomon et al., 2011). Given its important impact on the ozone layer and climate it is unfortunate that the sources of sulfate aerosol are not better characterized. Chin and Davis (1995) constructed a one-dimensional photochemical model of the stratosphere and found that OCS could explain between 20 % and 50 % of background production of SSA. A later study by Pitari et al. (2002) found it to be 43 %. Engel and Schmidt (1994) found that most background SSA was produced by stratospheric oxidation of OCS. In contrast, Leung et al. (2002) concluded that either OCS is a minor contributor to SSA or that the current understanding of the  $^{34}\text{S}$  abundance in SSA and atmospheric circulation are seriously flawed. The very recent study by Brühl et al. (2012) found evidence that OCS plays a controlling role in the production of background SSA but was not able to

## Isotopic fractionation of stratospheric OCS

J. A. Schmidt et al.

Title Page

Abstract

Introduction

Conclusions

References

Tables

Figures

◀

▶

◀

▶

Back

Close

Full Screen / Esc

Printer-friendly Version

Interactive Discussion



give a quantitative figure, although they found that the OCS to SSA conversion rate is about  $0.035 \text{ MtSyr}^{-1}$  in good agreement with the results of Chin and Davis (1995).

In a series of papers we use stable isotope analysis to trace the stratospheric sulfur cycle (Hattori et al., 2011, 2012; Schmidt et al., 2012a). Physical and chemical processes can alter stable isotope abundances in a given sample. Isotopic analysis is therefore used to trace the sources, sinks and transformations of atmospheric trace gases, cf. Johnson et al. (2002). A compound's sources and sinks are linked via the mass balance equation. Newman et al. (1991) estimated that tropospheric OCS carries a small enrichment in  $^{34}\text{S}$  ( $\delta^{34}\text{S}=11 \text{ ‰}$ ). Castleman et al. (1974) measured an even smaller  $^{34}\text{S}$  enrichment in SSA ( $\delta^{34}\text{S}=2.6 \text{ ‰}$ ). These enrichments were reported relative to standard meteoritic sulfur ( $^{34}\text{S}/^{32}\text{S}=0.0450248$ ). Leung et al. (2002) retrieved  $\text{OC}^{32}\text{S}$  and  $\text{OC}^{34}\text{S}$  concentrations as a function of altitude from data acquired using the NASA Jet Propulsion Laboratory MkIV Fourier Transform Infra-Red (FTIR) Spectrometer. The concentration profiles showed a very large  $^{34}\text{S}$  depletion in the stratosphere. Based on this finding and the small observed  $^{34}\text{S}$  depletion in SSA relative to tropospheric OCS, it was concluded that OCS is not a significant source of SSA. A later study by the same group found OCS photolysis in the first UV-band gives a large  $^{34}\text{S}$  depletion in the remaining OCS (Colussi et al., 2004). The latter result is contradicted by the recent results of Hattori et al. (2011) and Lin et al. (2011) which found that OCS photolysis produces only very small depletion or even enrichment of  $^{34}\text{S}$  in the remaining pool of OCS.

There have only been a few theoretical studies of the OCS photolysis isotope effects. Jørgensen et al. (2008) used the potential energy surfaces of Suzuki et al. (1998) and found the  $^{34}\text{S}$  enrichment to be very small. A similar result was obtained by Danielache et al. (2009) using different potential energy surfaces. The latter study also considered  $^{13}\text{C}$  fractionation and found photolysis to greatly deplete OCS in  $^{13}\text{C}$  which contradicts recent experimental results of Hattori et al. (2011).

In this study we: (i) calculate the OCS,  $\text{OC}^{33}\text{S}$ ,  $\text{OC}^{34}\text{S}$ ,  $\text{OC}^{36}\text{S}$  and  $\text{O}^{13}\text{CS}$  absorption cross sections and derive isotopic fractionation factors at different temperatures.

## Isotopic fractionation of stratospheric OCS

J. A. Schmidt et al.

Title Page

Abstract

Introduction

Conclusions

References

Tables

Figures

◀

▶

◀

▶

Back

Close

Full Screen / Esc

Printer-friendly Version

Interactive Discussion



(ii) Determine the potential for non-mass-dependent fractionation and (iii) determine an overall  $^{34}\text{S}$  isotopic fractionation constant for the stratosphere by also considering isotopic fractionation in the atomic oxygen and hydroxyl radical sink reactions (Hattori et al., 2012; Schmidt et al., 2012a).

## 2 Methodology

The absorption cross section is a central quantity in photochemistry. It can be calculated from first principles by first constructing potential energy surfaces for the relevant electronic states (by solving the electronic Schrödinger equation) and then solving the time-dependent Schrödinger equation for the nuclear motion on the surfaces (Schinke, 1993, Chap. 4). This procedure was used by Schmidt et al. (2009, 2011) to describe isotopic fraction in HCl and  $\text{N}_2\text{O}$  photolysis. OCS photodissociation is a multi-state process involving both singlet and triplet states (Schmidt et al., 2012b,c). In what follows, the electronic states  $1^1A'$ ,  $2^1A'$ ,  $1^1A''$ , and  $2^1A''$  will be termed X, A, B, and C, respectively, and the triplet states  $1^3A'$ ,  $1^3A''$ ,  $2^3A''$ , and  $2^3A'$  will be referred to as a, b, c, and d.

### 2.1 Potential energy surfaces

The potential energy surfaces (PES) for the lowest four singlet states and lowest four triplet states were calculated using the multi-configuration reference internally contracted configuration interaction (MRCI) theory (Werner and Knowles, 1988; Knowles and Werner, 1988) based on wave functions obtained by state-averaged full-valence complete active space self consistent field (CASSCF) calculations (Werner and Knowles, 1985; Knowles and Werner, 1985). The 7 core orbitals were kept frozen during the MRCI calculations. The augmented correlation consistent polarized valence quadruple zeta (aug-cc-pVQZ) basis set of Dunning Jr. (1989) was employed. The Davidson correction was applied in order to approximately account for contributions

## Isotopic fractionation of stratospheric OCS

J. A. Schmidt et al.

Title Page

Abstract

Introduction

Conclusions

References

Tables

Figures

◀

▶

◀

▶

Back

Close

Full Screen / Esc

Printer-friendly Version

Interactive Discussion



of higher excitations and for size-extensive energies (Langhoff and Davidson, 1974). The corresponding transition dipole moment (TDM) functions for transitions between the ground state and excited singlet states were calculated at the same level of theory but with the aug-cc-pVTZ basis set. The PESs and the TDM were calculated as functions of the Jacobi coordinates  $R$  (distance from S to the center of mass of CO),  $r$  (CO bond length), and  $\gamma$  (angle between  $R$  and  $r$ ). The TDMs connecting the singlet ground state to the triplet states were calculated as functions of  $\gamma$  only. Further details are given by Schmidt et al. (2012b,c). For isotopomers including different carbon isotopes a coordinate transformation between the different sets of Jacobi coordinates is mandatory.

These PESs and TDMs are currently the most accurate ab initio surfaces available for OCS. They are the first set of surfaces to successfully describe the first UV absorption band of carbonyl sulfide including the superimposed structure near the peak of the band and the weak structure observed at longer wavelengths at the onset of the band (Schmidt et al., 2012b,c).

## 2.2 Quantum mechanical calculations

The absorption cross sections for OCS, OC<sup>33</sup>S, OC<sup>34</sup>S, OC<sup>36</sup>S and O<sup>13</sup>CS were calculated using the time-dependent approach (Schinke, 1993), i.e. by propagating a quantum mechanical wave packet  $\Phi(t)$  and Fourier transforming the resulting autocorrelation function  $S(t) = \langle \Phi(0) | \Phi(t) \rangle$ . The wave packets at  $t = 0$  were defined as the product of the modulus of the TDM and a vibrational wave function of the X state. The six lowest vibrational states were included in the analysis. The temperature dependent cross section for excitation from the electronic ground state into a particular excited electronic state was obtained by Boltzmann averaging over all initial vibrational states including a  $(v_2 + 1)$  pseudo degeneracy factor. Finally, summation of the cross sections for states A, B, C, a, b, c, and d yielded the total cross section for a given temperature  $T$ .

The details of the calculations and the methodology are almost identical to those given by Schmidt et al. (2012c). The only difference is the grid parameters: in this

### Isotopic fractionation of stratospheric OCS

J. A. Schmidt et al.

Title Page

Abstract

Introduction

Conclusions

References

Tables

Figures

◀

▶

◀

▶

Back

Close

Full Screen / Esc

Printer-friendly Version

Interactive Discussion



study the wave packets were represented on a three-dimensional grid with 250 points for  $3 a_0 \leq R \leq 10 a_0$ , 70 points for  $1.6 a_0 \leq r \leq 3.6 a_0$ , and 200 points for  $0 \leq \gamma \leq \pi$ .

Note that the experimental fractionation constants shown in this study were averaged using a moving Gaussian with full width at half maximum of  $200 \text{ cm}^{-1}$  (approximately 1 nm). This damped the noise induced by oscillations at longer and shorter wavelengths. The theoretical results were averaged using the same procedure.

### 2.3 Photochemical calculations

The rate of photolysis,  $j$ , under different experimental conditions or at different altitudes in the atmosphere can be calculated from the following integral,

$$j = \int d\lambda \sigma(\lambda) F(\lambda) \phi(\lambda), \quad (1)$$

where  $F(\lambda)$  is the quantity of light available for photolysis at given wavelength, e.g. the actinic flux in the case of atmospheric photolysis. The yield of dissociation,  $\phi(\lambda)$ , is set to unity. Actinic flux data at 0.01 nm resolution at various altitudes were obtained from McLinden et al. (2002).

### 2.4 Isotopic fractionation

The enrichment of a given isotope, e.g.  $^{34}\text{S}$ , is quantified in terms of the relative isotope ratio difference (or isotope delta) defined as,

$$\delta^{34}\text{S} = \frac{{}^{34}R}{{}^{34}R_{\text{ref}}} - 1, \quad (2)$$

where  ${}^{34}R_{\text{ref}}$  is the  $^{34}\text{S} : {}^{32}\text{S}$  ratio in a reference, with Vienna Canyon Diablo Troilite (VCDT) being the accepted reference for sulfur ( ${}^{34}R_{\text{VCDT}} = 0.0441626$ ). A relative isotope ratio difference for carbon-13 ( $\delta^{13}\text{C}$ ) is defined in a similar way.

## Isotopic fractionation of stratospheric OCS

J. A. Schmidt et al.

Title Page

Abstract

Introduction

Conclusions

References

Tables

Figures

◀

▶

◀

▶

Back

Close

Full Screen / Esc

Printer-friendly Version

Interactive Discussion



The OC<sup>34</sup>S isotopic fractionation as function of wavelength is commonly quantified using the *fractionation constant* (cf. Danielache et al., 2009; Hattori et al., 2011),

$${}^{34}\epsilon(\lambda) = \frac{{}^{34}\sigma(\lambda)}{\sigma(\lambda)} - 1, \quad (3)$$

where  $\sigma(\lambda)$  and  ${}^{34}\sigma(\lambda)$  are the OC<sup>32</sup>S and OC<sup>34</sup>S cross sections respectively, and analogous definitions apply for the other isotopes. The effective fractionation constant can also be defined for specific photolysis conditions using,

$${}^{34}e = \frac{{}^{34}j}{j} - 1. \quad (4)$$

Following Ueno et al. (2009) and Hattori et al. (2011) we also introduce the quantities  ${}^{33}E$  and  ${}^{36}E$  for describing departures from mass-dependent fractionation,

$${}^iE = {}^ie + 1 - \left({}^{34}e + 1\right)^{\beta_i}, \quad (5)$$

with  $i = 33$  or  $36$ ,  $\beta_{33} = 0.515$  and  $\beta_{36} = 1.90$ .

### 3 Results and comparison with experiments

Table 1 lists calculated vibrational energies and deviations from experimental results for 5 different isotopologues. The absolute deviation between theory and experiment is small; the vibrational energies deviate from experimental values by at most 0.9%. Furthermore, the deviation is roughly the same for all isotopologues i.e., the shift in energy with isotopic substitution is very well reproduced.

The calculated cross section for the most abundant OCS isotopologue is shown in Fig. 1 and compared with the low-temperature experimental cross section of Robert

## Isotopic fractionation of stratospheric OCS

J. A. Schmidt et al.

Title Page

Abstract

Introduction

Conclusions

References

Tables

Figures

◀

▶

◀

▶

Back

Close

Full Screen / Esc

Printer-friendly Version

Interactive Discussion



Wu et al. (1999). Note that when summing over all the seven excited electronic states the A-state cross sections for all initial states ( $\nu_1, \nu_2, \nu_3$ ) were shifted by  $200 \text{ cm}^{-1}$  to higher energies; all the other cross sections remained unshifted. This shift is less than 0.5% of the transition energy and is mainly due to computational error in the relative placement of the A-state surface. This shift was also applied in our previous theoretical studies (Schmidt et al., 2012b,c). Probably due to inaccuracies of the TDMs the calculated cross section is about 30% smaller than the measured one and therefore it was multiplied by 1.3 in Fig. 1; a similar deviation was observed for  $\text{N}_2\text{O}$  (Schinke et al., 2010; Schinke, 2011). Overall, the theoretical and experimental cross sections are in good agreement including the width of the broad continuum and the positions and intensities of the superimposed structures.

### 3.1 Photolytic isotope effects

Figure 2 shows the theoretical fractionation constants compared with experimental results of Hattori et al. (2011). The experimental data of Hattori et al. (2011) were recorded with a spectral resolution of 0.1 nm and in intervals of 0.02 nm while the theoretical data was calculated in intervals of  $1 \text{ cm}^{-1}$  (approximately 0.01 nm). To ease comparison the resolution of both experimental and theoretical cross sections were degraded by applying a moving Gaussian average with FWHM of  $200 \text{ cm}^{-1}$ . This averaged out the noise in the experimental cross sections at  $\lambda > 240 \text{ nm}$  and  $\lambda < 210 \text{ nm}$ . Overall, the agreement between experiment and theory is excellent. The theoretical fractionation constants tend to be more structured at shorter wavelengths than observed in the experiment. The theoretical cross section (Fig. 1) also shows slightly too much structure on the high energy side. The sulfur isotope fractionation is small in the stratospheric UV window ( $\sim 190 - 220 \text{ nm}$ ) but becomes more negative at longer wavelengths. The position, intensity and frequency of structure in the calculations agree well with experimental results. The  $^{13}\text{C}$  fractionation constant ( $^{13}\epsilon$ ) is more negative than  $^{34}\epsilon$ , reflecting the larger relative change in mass. Furthermore isotopic substitution of the central C atom has a larger effect on the bending degree of freedom (see Table 1)

## Isotopic fractionation of stratospheric OCS

J. A. Schmidt et al.

Title Page

Abstract

Introduction

Conclusions

References

Tables

Figures



Back

Close

Full Screen / Esc

Printer-friendly Version

Interactive Discussion



and the vibrational wavefunction of  $O^{13}CS$  becomes more localized around linearity where the TDM is small thus lowering the overall cross section.

Since the vibrational wavefunctions of the heavy isotopologues of OCS tend to be more localized around linearity (i.e. more narrow) the cross sections for these isotopologues will be smaller than that of light OCS. A similar effect is seen in  $N_2O$  (Johnson et al., 2001). The smaller cross section leads to an overall negative fractionation constant. This contradicts the claims presented by Colussi et al. (2004) who stated that a positive  $^{34}S$  fractionation constant was to be expected from theory.

For direct dissociation, where the absorption cross section is characterized by a broad continuum, substitution with a heavier isotope tends to make the cross section more narrow (due to a narrowing of the vibrational wavefunction, cf. Liang et al., 2004) and shift the cross section to higher energies (due a lowering of the vibrational zero point energy, cf. Yung and Miller, 1997). The change in the cross section with isotopic substitution is marginal near the center while it is significant on the shoulders. In particular, the cross sections for the heavy isotope tends to be smaller on the low energy side due to the narrowing of the ground state vibrational wave functions and lowering of the ground state vibrational energies. Stratospheric photolysis of OCS occurs near the center of the cross section where the fractionation constant is close to zero. In contrast,  $N_2O$  photolysis occurs on the low energy shoulder of the cross section giving rise to a large enrichment of heavy  $N_2O$  in the stratosphere (Kim and Craig, 1993; Rahn and Wahlen, 1997; Toyoda et al., 2001; Röckmann et al., 2001; Prakash et al., 2005; Chen et al., 2008, 2010).

Figure 3 shows the calculated  $^{33}E$  and  $^{36}E$  compared to the experimental results of Hattori et al. (2011). The calculated  $^{33}E$  is very close to 0 ‰ and shows marginal structure while the experimental  $^{33}E$  is zero at long wavelengths but shows a negative trend with decreasing wavelength; however, theory and experiment generally agree to within the experimental uncertainty. The calculated  $^{36}E$  is shown in panel (b) of Fig. 3; note that no wavelength resolved experimental data is available for  $^{36}E$ . Both  $^{33}E$  and  $^{36}E$  are almost unaffected by cooling from 295 K to 220 K.

## Isotopic fractionation of stratospheric OCS

J. A. Schmidt et al.

[Title Page](#)[Abstract](#)[Introduction](#)[Conclusions](#)[References](#)[Tables](#)[Figures](#)[⏪](#)[⏩](#)[◀](#)[▶](#)[Back](#)[Close](#)[Full Screen / Esc](#)[Printer-friendly Version](#)[Interactive Discussion](#)

## 3.2 Atmospheric implications

The isotopic fractionation of OCS photolysis in the tropopause and stratosphere of the US standard atmosphere was calculated using the actinic flux data of McLinden et al. (2002) (Fig. 4) together with Eq. (1) and is given in Fig. 5. The  $^{34}\text{S}$  fractionation constant grows rapidly below 15 km while the rate of photolysis decreases rapidly due to the low level of stratospheric UV radiation. Above 15 km the  $^{34}\text{S}$  fractionation constant is close to zero; between 18 and 30 km it is slightly negative while it becomes slightly positive above 30 km. The  $^{33}\text{S}$  and  $^{36}\text{S}$  fractionation constants (not shown) are qualitatively similar. The  $^{13}\text{C}$  isotopic fraction is negative above 16 km and becomes increasingly negative with increasing altitude.

Figure 5 also shows  $^{33}E$  and  $^{36}E$  as function of  $z$ . At altitudes above 20 km  $^{33}E$  and  $^{36}E$  are both close to 0 and photolysis is mass-dependent. At altitudes below 20 km  $^{33}E$  and  $^{36}E$  start to diverge in opposite directions giving non-mass-dependent fractionation. Below 20 km the UV window is narrow and sharp ( $\sim 205$  to  $212$  nm, see Fig. 4) and photodissociation primarily occurs in a narrow region on the high energy shoulder of the cross section. The narrow window creates a situation where the vibrational structure of the cross sections of the different isotopologues can lie just inside or just outside the window, “opening the door” for non-mass-dependent fractionation. Unfortunately the window is centered in the region where the calculated cross section is too structured compared to experiment. The very sharp cutoff of the actinic flux below 205 nm is due to absorption by  $\text{O}_2$ .

A simple “pen-and-paper” chemical box model was constructed to get an integrated picture of isotopic fractionation caused by the OCS stratospheric sink reactions. The results of the model and the input parameters are shown in Table 2 for three different altitudes. When calculating the total lifetime of OCS against the sinks  $j_{\text{ph}}$ ,  $[\text{O}]$  and  $[\text{OH}]$  were scaled by a factor of  $\frac{1}{4}$  to get a global day/night average of the photolysis rate and effective O and OH concentrations. The combined  $^{34}\text{S}$  fractionation of the three sink reactions is small and negative at the three altitudes. It is difficult to reconcile the total

### Isotopic fractionation of stratospheric OCS

J. A. Schmidt et al.

Title Page

Abstract

Introduction

Conclusions

References

Tables

Figures



Back

Close

Full Screen / Esc

Printer-friendly Version

Interactive Discussion



## Isotopic fractionation of stratospheric OCS

J. A. Schmidt et al.

Title Page

Abstract

Introduction

Conclusions

References

Tables

Figures

◀

▶

◀

▶

Back

Close

Full Screen / Esc

Printer-friendly Version

Interactive Discussion



<sup>34</sup>S fractionation constant of our study (second last line of Table 2) with the value of  $^{34}\epsilon = (73.8 \pm 8.6) \text{‰}$  presented by Leung et al. (2002) for the stratosphere. The large stratospheric fractionation constant was suggested to be due to photolysis and Colussi et al. (2004) did indeed find photolysis to have a large positive fractionation constant of  $^{34}\epsilon = (67 \pm 7) \text{‰}$ , however our results and recent studies suggest that the photolytic <sup>34</sup>S fractionation constant in general is much smaller and negative (Hattori et al., 2011; Lin et al., 2011).

The <sup>13</sup>C fractionation in the stratosphere is also negative but has a larger magnitude. The magnitude of  $^{13}\epsilon$  increases with altitude. The larger isotopic fractionation for <sup>13</sup>C may produce a strong enough signal in the OCS isotopic record to be detected and traced using the ACE-FTS or MIPAS data sets leading to a better quantification of background SSA, which is important input to climate models (Myhre et al., 2004; Solomon et al., 2011).

## 4 Conclusions

In this study we found:

1. OCS photolytic <sup>34</sup>S isotopic fractionation is marginal validating recent studies by Hattori et al. (2011) and Lin et al. (2011) while directly contradicting the findings of Colussi et al. (2004).
2. The overall <sup>34</sup>S isotopic fractionation of OCS in the stratosphere is small and negative which contradicts the findings of Leung et al. (2002) and makes OCS an acceptable source of background SSA in agreement with a recent model study of Brühl et al. (2012).
3. <sup>13</sup>C fractionation of stratospheric OCS is significant and becomes increasingly negative with altitude which makes <sup>13</sup>C a promising tracer candidate for the ACE-FTS and MIPAS data sets.

4. The O sink reaction is more fractionating than stratospheric photolysis and the OH reaction which opens an opportunity for constructing a more detailed stratospheric OCS budget.

5 The data at hand allows for a detailed photochemical model a la McLinden et al. (2003) to be set up. However more field/remote sensing studies are needed to get better values for the isotopic composition of SSA and tropospheric and stratospheric OCS.

10 *Acknowledgements.* We thank Chris McLinden for providing us with the actinic flux data. We thank the IntraMIF project in the European Community's Seventh Framework Programme (FP7/2007-2013) under grant agreement number 237890 for support. We thank the Gesellschaft für wissenschaftliche Datenverarbeitung mbH Göttingen (GWDG) for computational resources. This work is supported by Grant in Aid for Scientific Research (S) (23224013) of Ministry of Education, Culture, Sports, and Technology (MEXT), Japan. S. H. is supported by Grant in Aid for JSPS Research Fellows (DC1(No. 22-7563)) and Global COE program "the Earth to Earths" of MEXT, Japan.

## References

- 15 Barkley, M. P., Palmer, P. I., Boone, C. D., Bernath, P. F., and Suntharalingam, P.: Global distributions of carbonyl sulfide in the upper troposphere and stratosphere, *Geophys. Res. Lett.*, 35, L14810, doi:10.1029/2008GL034270, 2008. 25330, 25331, 25348
- 20 Belafhal, A., Fayt, A., and Guelachvili, G.: Fourier transform spectroscopy of carbonyl sulfide from 1800 to 3120 cm<sup>-1</sup>: the normal species, *J. Mol. Struct.*, 174, 1–19, doi:10.1006/jmsp.1995.1264, 1995. 25347
- 25 Belviso, S., Mihalopoulos, N., and Nguyen, B. C.: The supersaturation of carbonyl sulfide (OCS) in rain waters, *Atmos. Environ.*, 21, 1363–1367, doi:10.1016/0004-6981(67)90083-2, 1967. 25330
- Brühl, C., Lelieveld, J., Crutzen, P. J., and Tost, H.: The role of carbonyl sulphide as a source of stratospheric sulphate aerosol and its impact on climate, *Atmos. Chem. Phys.*, 12, 1239–1253, doi:10.5194/acp-12-1239-2012, 2012. 25330, 25331, 25340

## Isotopic fractionation of stratospheric OCS

J. A. Schmidt et al.

Title Page

Abstract

Introduction

Conclusions

References

Tables

Figures

◀

▶

◀

▶

Back

Close

Full Screen / Esc

Printer-friendly Version

Interactive Discussion



**Isotopic  
fractionation of  
stratospheric OCS**

J. A. Schmidt et al.

Title Page

Abstract

Introduction

Conclusions

References

Tables

Figures

◀

▶

◀

▶

Back

Close

Full Screen / Esc

Printer-friendly Version

Interactive Discussion



Castleman, A. W., Munkelwitz, H. R., and Manowitz, B.: Isotopic studies of the sulfur component of the stratospheric aerosol layer, *Tellus B*, 26, 222–234, available at: <http://www.tellusb.net/index.php/tellusb/article/view/13739/15505>, 1974. 25332

Chen, W.-C., Prakash, M. K., and Marcus, R. A.: Isotopomer fractionation in the UV photolysis of  $N_2O$ : 2. Further comparison of theory and experiment, *J. Geophys. Res.*, 113, D05309, doi:10.1029/2007JD009180, 2008. 25338

Chen, W.-C., Nanbu, S., and Marcus, R. A.: Isotopomer fractionation in the UV photolysis of  $N_2O$ : 3. 3-D ab initio surfaces and anharmonic effects, *J. Phys. Chem. A*, 114, 9700–9708, doi:10.1021/jp101691r, 2010. 25338

Chin, M. and Davis, D. D.: A reanalysis of carbonyl sulfide as a source of stratospheric background sulfur aerosol, *J. Geophys. Res.*, 100, 8993–9005, doi:10.1029/95JD00275, 1995. 25330, 25331, 25332

Colussi, A. J., Leung, F., and Hoffmann, M. R.: Electronic spectra of carbonyl sulfide sulfur isotopologues, *Environ. Chem.*, 1, 44–48, doi:10.1071/EN04010, 2004. 25332, 25338, 25340

Crutzen, P. J.: The possible importance of CSO for the sulfate layer of the stratosphere, *Geophys. Res. Lett.*, 3, 73–76, doi:10.1029/GL003i002p00073, 1976. 25331

Danielache, S. O., Nanbu, S., Eskebjerg, C., Johnson, M. S., and Yoshida, N.: Carbonyl sulfide isotopologues: ultraviolet absorption cross sections and stratospheric photolysis, *J. Chem. Phys.*, 131, 024307, doi:10.1063/1.3156314, 2009. 25332, 25336

Dunning Jr., T. H.: Gaussian basis sets for use in correlated molecular calculations. I. The atoms boron through neon and hydrogen, *J. Chem. Phys.*, 90, 1007–1023, doi:10.1063/1.456153, 1989. 25333

Engel, A. and Schmidt, U.: Vertical profile measurements of carbonylsulfide in the stratosphere, *Geophys. Res. Lett.*, 21, 2219–2222, doi:10.1029/94GL01461, 1994. 25331

Hattori, S., Danielache, S. O., Johnson, M. S., Schmidt, J. A., Kjaergaard, H. G., Toyoda, S., Ueno, Y., and Yoshida, N.: Ultraviolet absorption cross sections of carbonyl sulfide isotopologues  $OC^{32}S$ ,  $OC^{33}S$ ,  $OC^{34}S$  and  $O^{13}CS$ : isotopic fractionation in photolysis and atmospheric implications, *Atmos. Chem. Phys.*, 11, 10293–10303, doi:10.5194/acp-11-10293-2011, 2011. 25330, 25332, 25336, 25337, 25338, 25340, 25350, 25351

Hattori, S., Schmidt, J. A., Mahler, D. W., Danielache, S. O., Johnson, M. S., and Yoshida, N.: Isotope effect in the carbonyl sulfide reaction with  $O(3P)$ , *J. Phys. Chem. A*, 116, 3521–3526, doi:10.1021/jp2120884, 2012. 25332, 25333, 25348

**Isotopic  
fractionation of  
stratospheric OCS**

J. A. Schmidt et al.

Title Page

Abstract

Introduction

Conclusions

References

Tables

Figures

◀

▶

◀

▶

Back

Close

Full Screen / Esc

Printer-friendly Version

Interactive Discussion



- Hofmann, D. J.: Increase in the stratospheric background sulfuric acid aerosol mass in the past 10 years, *Science*, 248, 996–1000, doi:10.1126/science.248.4958.996, 1990. 25331
- Johnson, M. S., Billing, G. D., Gruodis, A., and Janssen, M. H. M.: Photolysis of nitrous oxide isotopomers studied by time-dependent hermite propagation, *J. Phys. Chem. A*, 105, 8672–8680, doi:10.1021/jp011449x, 2001. 25338
- Johnson, M. S., Feilberg, K. L., Hessberg, P. v., and Nielsen, O. J.: Isotopic processes in atmospheric chemistry, *Chem. Soc. Rev.*, 31, 313–323, doi:10.1039/B108011N, 2002. 25332
- Jørgensen, S., Grage, M. M.-L., Nyman, G., and Johnson, M. S.: Chapter 7 isotope effects in photodissociation: chemical reaction dynamics and implications for atmospheres, in: *Applications of Theoretical Methods to Atmospheric Science*, *Adv. Quantum Chem.*, 55, 101–135, doi:10.1016/S0065-3276(07)00207-9, 2008. 25332
- Kim, K.-R. and Craig, H.: Nitrogen-15 and oxygen-18 characteristics of nitrous oxide: a global perspective, *Science*, 262, 1855–1857, doi:10.1126/science.262.5141.1855, 1993. 25338
- Knowles, P. J. and Werner, H.-J.: An efficient second-order MC SCF method for long configuration expansions, *Chem. Phys. Lett.*, 115, 259–267, doi:10.1016/0009-2614(85)80025-7, 1985. 25333
- Knowles, P. J. and Werner, H.-J.: An efficient method for the evaluation of coupling coefficients in configuration interaction calculations, *Chem. Phys. Lett.*, 145, 514–522, doi:10.1016/0009-2614(88)87412-8, 1988. 25333
- Langhoff, S. R. and Davidson, E. R.: Configuration interaction calculations on the nitrogen molecule, *J. Quantum Chem.*, 8, 61–72, doi:10.1002/qua.560080106, 1974. 25334
- Leung, F., Colussi, A. J., and Hoffmann, M. R.: Isotopic fractionation of carbonyl sulfide in the atmosphere: Implications for the source of background stratospheric sulfate aerosol, *Geophys. Res. Lett.*, 29, 1474, doi:10.1029/2001GL013955, 2002. 25330, 25331, 25332, 25340
- Liang, M.-C., Blake, G. A., and Yung, Y. L.: A semianalytic model for photo-induced isotopic fractionation in simple molecules, *J. Geophys. Res.*, 109, D10308, doi:10.1029/2004JD004539, 2004. 25338
- Lin, Y., Sim, M. S., and Ono, S.: Multiple-sulfur isotope effects during photolysis of carbonyl sulfide, *Atmos. Chem. Phys.*, 11, 10283–10292, doi:10.5194/acp-11-10283-2011, 2011. 25332, 25340
- McLinden, C. A., McConnell, J. C., Griffioen, E., and McElroy, C. T.: A vector radiative-transfer model for the Odin/OSIRIS project, *Can. J. Phys.*, 80, 375–393, doi:10.1139/p01-156, 2002. 25335, 25339, 25352, 25353

**Isotopic  
fractionation of  
stratospheric OCS**

J. A. Schmidt et al.

Title Page

Abstract

Introduction

Conclusions

References

Tables

Figures

◀

▶

◀

▶

Back

Close

Full Screen / Esc

Printer-friendly Version

Interactive Discussion



McLinden, C. A., Prather, M. J., and Johnson, M. S.: Global modeling of the isotopic analogues of N<sub>2</sub>O: Stratospheric distributions, budgets, and the <sup>17</sup>O-<sup>18</sup>O mass-independent anomaly, *J. Geophys. Res.*, 108, 4233, doi:10.1029/2002JD002560, 2003. 25341

Montzka, S. A., Calvert, P., Hall, B. D., Elkins, J. W., Conway, T. J., Tans, P. P., and Sweeney, C.: On the global distribution, seasonality, and budget of atmospheric carbonyl sulfide (COS) and some similarities to CO<sub>2</sub>, *J. Geophys. Res.*, 112, D09302, doi:10.1029/2006JD007665, 2007. 25330, 25331

Myhre, G., Berglen, T. F., Myhre, C. E. L., and Isaksen, I. S.: The radiative effect of the anthropogenic influence on the stratospheric sulfate aerosol layer, *Tellus B*, 56, 294–299, doi:10.1111/j.1600-0889.2004.00106.x, 2004. 25331, 25340

Newman, L., Krouse, H. R., and Grinenko, V. A.: Chapter 5: Sulphur isotope variations atmosphere, in: *Stable Isotopes in the Assessment of Natural and Anthropogenic Sulphur in the Environment*, edited by: Krouse, H. R. and Grinenko, V. A., vol. 43 of SCOPE, John Wiley & Sons Ltd, <http://www.icsu-scope.org/downloadpubs/scope43/index.html>, 133–176, 1991. 25332

Notholt, J., Kuang, Z., Rinsland, C. P., Toon, G. C., Rex, M., Jones, N., Albrecht, T., Deckelmann, H., Krieg, J., Weinzierl, C., Bingemer, H., Weller, R., and Schrems, O.: Enhanced upper tropical tropospheric COS: impact on the stratospheric aerosol layer, *Science*, 300, 307–310, doi:10.1126/science.1080320, 2003. 25330

Pitari, G., Mancini, E., Rizi, V., and Shindell, D. T.: Impact of future climate and emission changes on stratospheric aerosols and ozone, *J. Atmos. Sci.*, 59, 414–440, doi:10.1175/1520-0469(2002)059<0414:IOFCAE>2.0.CO;2, 2002. 25331

Prakash, M. K., Weibel, J. D., and Marcus, R. A.: Isotopomer fractionation in the UV photolysis of N<sub>2</sub>O: comparison of theory and experiment, *J. Geophys. Res.*, 110, D21315, doi:10.1029/2005JD006127, 2005. 25338

Rahn, T. and Wahlen, M.: Stable isotope enrichment in stratospheric nitrous oxide, *Science*, 278, 1776–1778, doi:10.1126/science.278.5344.1776, 1997. 25338

Robert Wu, C. Y., Chen, F. Z., and Judge, D. L.: Temperature-dependent photoabsorption cross sections of OCS in the 2000–2600 Å Region, *J. Quant. Spectrosc. Ra.*, 61, 265–271, doi:10.1016/S0022-4073(97)00220-3, 1999. 25336, 25349

Röckmann, T., Kaiser, J., Brenninkmeijer, C. A. M., Crowley, J. N., Borchers, R., Brand, W. A., and Crutzen, P. J.: Isotopic enrichment of nitrous oxide (<sup>15</sup>N<sup>14</sup>N<sup>16</sup>O, <sup>14</sup>N<sup>15</sup>N<sup>16</sup>O, <sup>14</sup>N<sup>14</sup>N<sup>18</sup>O)

**Isotopic  
fractionation of  
stratospheric OCS**

J. A. Schmidt et al.

Title Page

Abstract

Introduction

Conclusions

References

Tables

Figures

◀

▶

◀

▶

Back

Close

Full Screen / Esc

Printer-friendly Version

Interactive Discussion



in the stratosphere and in the laboratory, *J. Geophys. Res.*, 106, 10403–10410, doi:10.1029/2000JD900822, 2001. 25338

Schinke, R.: Photodissociation Dynamics, Cambridge University Press, New York, 1993. 25333, 25334

5 Schinke, R.: Photodissociation of N<sub>2</sub>O: potential energy surfaces and absorption spectrum, *J. Chem. Phys.*, 134, 064313, doi:10.1063/1.3553377, 2011. 25337

Schinke, R., Suarez, J., and Farantos, S. C.: Communication: photodissociation of N<sub>2</sub>O – frustrated NN bond breaking causes diffuse vibrational structures, *J. Chem. Phys.*, 133, 091103, doi:10.1063/1.3479391, 2010. 25337

10 Schmidt, J. A., Johnson, M. S., Grage, M. M.-L., and Nyman, G.: On the origin of the asymmetric shape of the HCl photodissociation cross section, *Chem. Phys. Lett.*, 480, 168–172, doi:10.1016/j.cplett.2009.09.014, 2009. 25333

Schmidt, J. A., Johnson, M. S., and Schinke, R.: Isotope effects in N<sub>2</sub>O photolysis from first principles, *Atmos. Chem. Phys.*, 11, 8965–8975, doi:10.5194/acp-11-8965-2011, 2011. 25333

15 Schmidt, J., Johnson, M., Jung, Y., Danielache, S., Hattori, S., and Yoshida, N.: Predictions of the sulfur and carbon kinetic isotope effects in the OH + OCS reaction, *Chem. Phys. Lett.*, 531, 64–69, doi:10.1016/j.cplett.2012.02.049, 2012a. 25332, 25333, 25348

Schmidt, J. A., Johnson, M. S., McBane, G. C., and Schinke, R.: Communication: multi-state analysis of the carbonyl sulfide ultraviolet absorption including vibrational structure, *J. Chem. Phys.*, 136, 131101, doi:10.1063/1.3701699, 2012b. 25333, 25334, 25337

20 Schmidt, J. A., Johnson, M. S., McBane, G. C., and Schinke, R.: The ultraviolet spectrum of OCS from first principles: electronic transitions, vibrational structure and temperature dependence, *J. Chem. Phys.*, 137, 054313, doi:10.1063/1.4739756, 2012c. 25333, 25334, 25337

25 Solomon, S., Sanders, R. W., Garcia, R. R., and Keys, J. G.: Increased chlorine dioxide over Antarctica caused by volcanic aerosols from Mount Pinatubo, *Nature*, 363, 245–248, doi:10.1038/363245a0, 1993. 25331

Solomon, S., Daniel, J. S., Neely, R. R., Vernier, J.-P., Dutton, E. G., and Thomason, L. W.: The persistently variable “background” stratospheric aerosol layer and global climate change, *Science*, 333, 866–870, doi:10.1126/science.1206027, 2011. 25331, 25340

30 Suzuki, T., Katayanagi, H., Nanbu, S., and Aoyagi, M.: Nonadiabatic bending dissociation in 16 valence electron system OCS, *J. Chem. Phys.*, 109, 5778–5794, doi:10.1063/1.477200, 1998. 25332

**Isotopic  
fractionation of  
stratospheric OCS**

J. A. Schmidt et al.

Title Page

Abstract

Introduction

Conclusions

References

Tables

Figures

◀

▶

◀

▶

Back

Close

Full Screen / Esc

Printer-friendly Version

Interactive Discussion



- Toyoda, S., Yoshida, N., Urabe, T., Aoki, S., Nakazawa, T., Sugawara, S., and Honda, H.: Fractionation of  $N_2O$  isotopomers in the stratosphere, *J. Geophys. Res.*, 106, 7515–7522, doi:10.1029/2000JD900680, 2001. 25338
- 5 Turco, R. P., Whitten, R. C., Toon, O. B., Pollack, J. B., and Hamill, P.: OCS, stratospheric aerosols and climate, *Nature*, 283, 283–285, doi:10.1038/283283a0, 1980. 25331
- Ueno, Y., Johnson, M. S., Danielache, S. O., Eskebjerg, C., Pandey, A., and Yoshida, N.: Geological sulfur isotopes indicate elevated OCS in the Archean atmosphere, solving faint young sun paradox, *P. Natl. Acad. Sci. USA*, 106, 14784–14789, doi:10.1073/pnas.0903518106, 2009. 25336
- 10 Watts, S. F.: The mass budgets of carbonyl sulfide, dimethyl sulfide, carbon disulfide and hydrogen sulfide, *Atmos. Environ.*, 34, 761–779, doi:10.1016/S1352-2310(99)00342-8, 2000. 25330, 25331
- Werner, H.-J. and Knowles, P. J.: A second order multiconfiguration SCF procedure with optimum convergence, *J. Chem. Phys.*, 82, 5053–5063, doi:10.1063/1.448627, 1985. 25333
- 15 Werner, H.-J. and Knowles, P. J.: An efficient internally contracted multiconfiguration–reference configuration interaction method, *J. Chem. Phys.*, 89, 5803–5814, doi:10.1063/1.455556, 1988. 25333
- Yung, Y. L. and Miller, C. E.: Isotopic fractionation of stratospheric nitrous oxide, *Science*, 278, 1778–1780, doi:10.1126/science.278.5344.1778, 1997. 25338
- 20 Zuniga, J., Bastida, A., Alacid, M., and Requena, A.: Excited vibrational states and potential energy function for OCS determined using generalized internal coordinates, *J. Chem. Phys.*, 113, 5695–5704, doi:10.1063/1.1290383, 2000. 25347

## Isotopic fractionation of stratospheric OCS

J. A. Schmidt et al.

**Table 1.** Vibrational excitation energies given in  $\text{cm}^{-1}$  for the different isotopologues, with  $E'_i = E_i - E_{(0,0,0)}$ . The numbers in parenthesis are  $E'_i(\text{calc}) - E'_i(\text{obs})$  with observed values taken from Belafhal et al. (1995) and Zuniga et al. (2000). ZPE is the calculated zero point vibrational energy.

	OCS	OC <sup>33</sup> S	OC <sup>34</sup> S	OC <sup>36</sup> S	O <sup>13</sup> CS
ZPE	1977.9	1974.3	1970.9	1964.7	1933.2
$E'_{(0,0,0)}$	0.0	0.0	0.0	0.0	0.0
$E'_{(0,1,0)}$	516.1 (−4.4) <sup>a</sup>	515.7	515.3	514.6	500.8
$E'_{(1,0,0)}$	852.7 (−6.3) <sup>b</sup>	847.0	841.5 (−6.2) <sup>b</sup>	831.5	848.2 (−6.2) <sup>b</sup>
$E'_{(0,2,0)}$	1038.2 (−8.8) <sup>b</sup>	1037.3	1036.4 (−8.8) <sup>b</sup>	1034.7	1007.7 (−8.5) <sup>b</sup>
$E'_{(1,1,0)}$	1361.8 (−10.6) <sup>a</sup>	1355.9	1350.2	1339.7	1342.1
$E'_{(0,3,0)}$	1560.3 (−13.1) <sup>a</sup>	1558.8	1557.3	1554.8	1514.4
$E'_{(2,0,0)}$	1698.4 (−12.6) <sup>b</sup>	1687.1	1676.3 (−12.4) <sup>b</sup>	1656.4	1689.3 (−12.5) <sup>b</sup>
$E'_{(1,2,0)}$	1877.4 (−14.9) <sup>b</sup>	1870.9	1864.9 (−14.8) <sup>b</sup>	1853.6	1842.5 (−14.5) <sup>b</sup>
$E'_{(0,0,1)}$	2050.8 (−11.4) <sup>b</sup>	2050.4	2050.0 (−11.4) <sup>b</sup>	2049.4	1997.9 (−11.3) <sup>b</sup>
$E'_{(0,4,0)}$	2087.7 (−17.1) <sup>b</sup>	2085.6	2083.6 (−17.0) <sup>b</sup>	2079.9	2026.8 (−16.3) <sup>b</sup>

<sup>a</sup> Belafhal et al. (1995)

<sup>b</sup> Zuniga et al. (2000)

Title Page

Abstract

Introduction

Conclusions

References

Tables

Figures

◀

▶

◀

▶

Back

Close

Full Screen / Esc

Printer-friendly Version

Interactive Discussion



**Table 2.** A very simple stratospheric model. Concentrations, rate constants and fractionation constants in the upper part of the table are used to derive the total stratospheric lifetime and fraction constants in the lower part of the table.

	16km	20km	24km	note
$T / \text{K}$	216.6	216.6	220.6	a
$p / \text{mbar}$	103.5	55.3	29.7	a
$n / 10^{18} \text{ cm}^{-3}$	3.46	1.85	0.98	a
$[\text{OCS}] / \text{ppt}$	310	180	110	b
$[\text{O}] / \text{ppt}$	0.3	1.6	10.2	c
$[\text{OH}] / \text{ppt}$	0.3	0.5	2.0	c
$j_{\text{ph}} / 10^{-9} \text{ s}^{-1}$	1.16	9.56	52.97	d
$k_{\text{O}} / 10^{-16} \text{ cm}^3 \text{ s}^{-1}$	8.15	8.15	9.80	c
$k_{\text{OH}} / 10^{-18} \text{ cm}^3 \text{ s}^{-1}$	5.51	4.40	4.45	f
$^{34}\epsilon_{\text{ph}} / \text{‰}$	4.2	-2.0	-2.1	d
$^{34}\epsilon_{\text{O}} / \text{‰}$	-21.7	-21.7	-21.7	e
$^{34}\epsilon_{\text{OH}} / \text{‰}$	-1.9	-3.7	-6.9	f
$^{13}\epsilon_{\text{ph}} / \text{‰}$	-2.9	-16.7	-18.9	d
$^{13}\epsilon_{\text{O}} / \text{‰}$	-17.0	-17.0	-16.6	g
$^{13}\epsilon_{\text{OH}} / \text{‰}$	-1.9	-3.7	-6.9	f
$\tau / \text{yr}$	64.0	10.6	2.0	h
$^{34}\epsilon_{\text{tot}} / \text{‰}$	-6.7	-6.0	-5.2	i
$^{13}\epsilon_{\text{tot}} / \text{‰}$	-8.8	-16.7	-18.5	i

<sup>a</sup> US standard atmosphere, <sup>b</sup> Fig. 4 in Barkley et al. (2008), <sup>c</sup> From JPL 2007 guide (40° N, noon), <sup>d</sup> This study using Eqs. (1) and (4) (equator at noon), <sup>e</sup> Hattori et al. (2012), <sup>f</sup> Schmidt et al. (2012a), <sup>g</sup> Calculated, see Hattori et al. (2012) for computational details, <sup>h</sup>  $\tau = 4 \cdot r_{\text{tot}}^{-1} = 4 \cdot (j_{\text{ph}} + k_{\text{O}}[\text{O}] + k_{\text{OH}}[\text{OH}])^{-1}$ . The factor of 4 is introduced to get an approximate global day/night average of  $j_{\text{ph}}$ ,  $[\text{O}]$  and  $[\text{OH}]$ , <sup>i</sup>  $\epsilon_{\text{tot}} = {}^x r_{\text{tot}} / r_{\text{tot}} - 1$  with  $x = 34$  or 13.

## Isotopic fractionation of stratospheric OCS

J. A. Schmidt et al.

Title Page

Abstract

Introduction

Conclusions

References

Tables

Figures

◀

▶

◀

▶

Back

Close

Full Screen / Esc

Printer-friendly Version

Interactive Discussion



## Isotopic fractionation of stratospheric OCS

J. A. Schmidt et al.

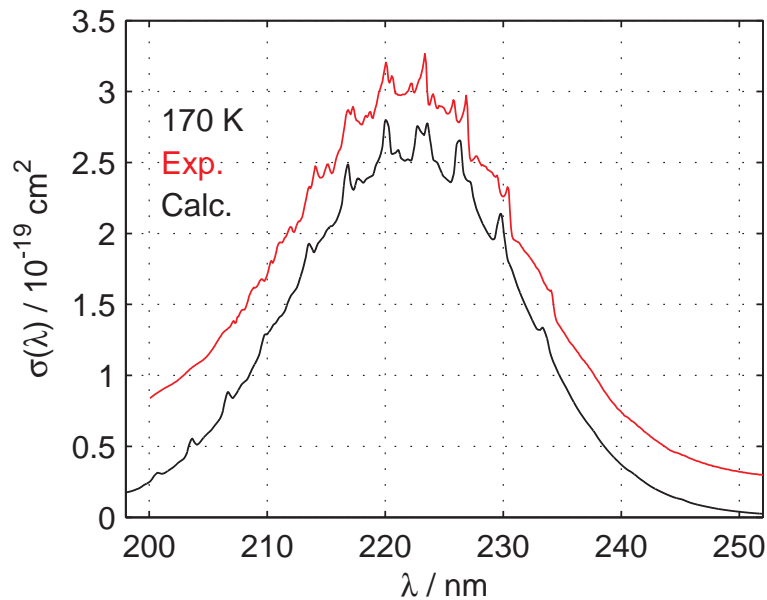


**Fig. 1.** The total absorption cross section (scaled by a factor of 1.3) compared with the experimental cross section of Robert Wu et al. (1999). The temperature in the calculation and measurement is 170 K. The experimental cross section was shifted up by 0.25 for clarity.

[Title Page](#)[Abstract](#)[Introduction](#)[Conclusions](#)[References](#)[Tables](#)[Figures](#)[◀](#)[▶](#)[◀](#)[▶](#)[Back](#)[Close](#)[Full Screen / Esc](#)[Printer-friendly Version](#)[Interactive Discussion](#)

## Isotopic fractionation of stratospheric OCS

J. A. Schmidt et al.

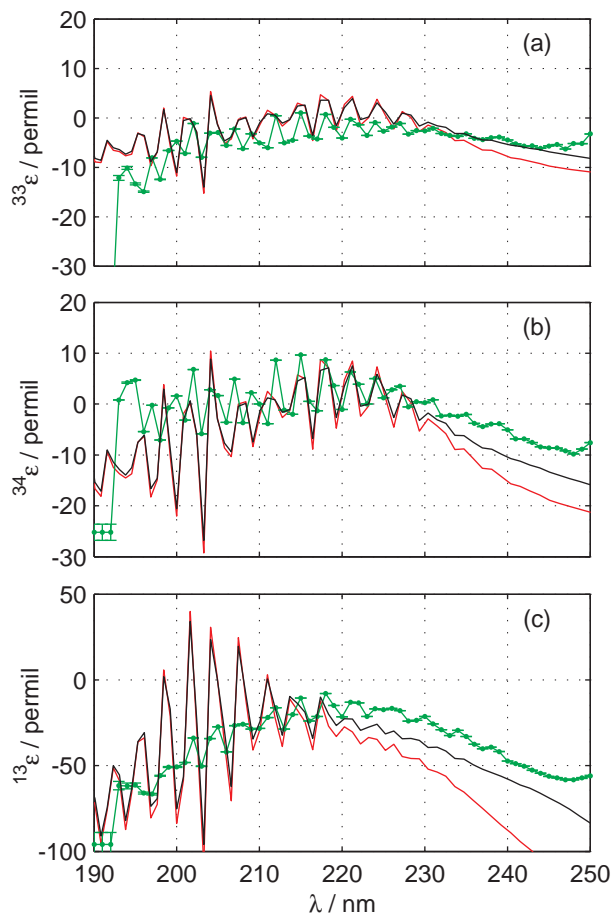


**Fig. 2.** (a) The calculated  $^{33}\text{S}$  fractionation constant vs. wavelength at 295 K (black) and 220 K (red) compared to the experimental  $^{33}\text{S}$  fractionation constant at room temperature (green) by Hattori et al. (2011). (b)  $^{34}\text{S}$  fractionation constant. (c)  $^{13}\text{C}$  fractionation constant.

Title Page

Abstract

Introduction

Conclusions

References

Tables

Figures

◀

▶

◀

▶

Back

Close

Full Screen / Esc

Printer-friendly Version

Interactive Discussion



## Isotopic fractionation of stratospheric OCS

J. A. Schmidt et al.

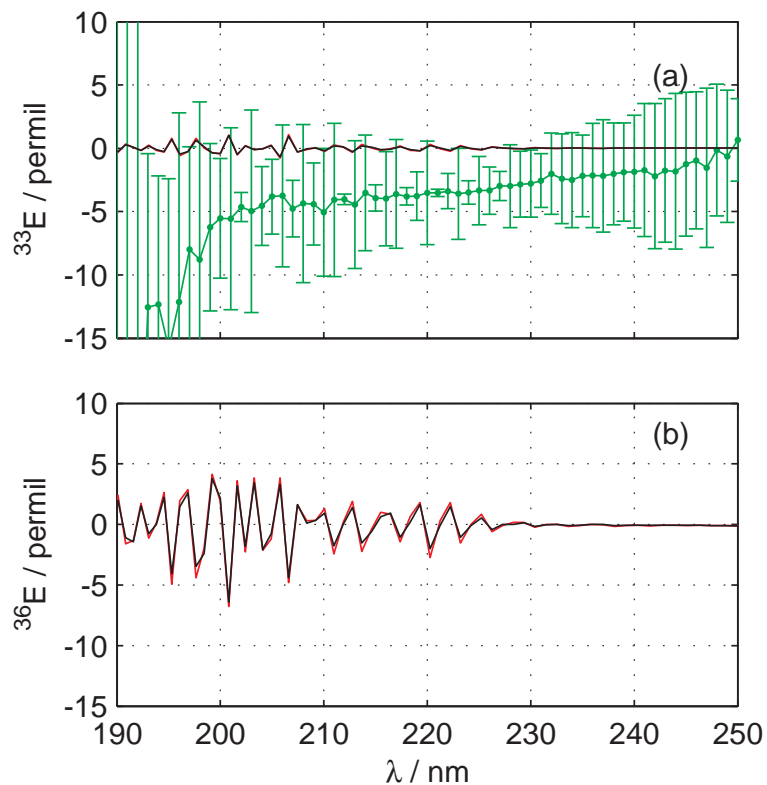


**Fig. 3.** (a) The calculated  $^{33}\text{E}$  vs. wavelength at 295 K (black) and 220 K (red) compared to the experimental results at room temperature (green) by Hattori et al. (2011). (b) The calculated  $^{36}\text{E}$  vs. wavelength at 295 K (black) and 220 K (red).

[Title Page](#)[Abstract](#)[Introduction](#)[Conclusions](#)[References](#)[Tables](#)[Figures](#)[◀](#)[▶](#)[◀](#)[▶](#)[Back](#)[Close](#)[Full Screen / Esc](#)[Printer-friendly Version](#)[Interactive Discussion](#)

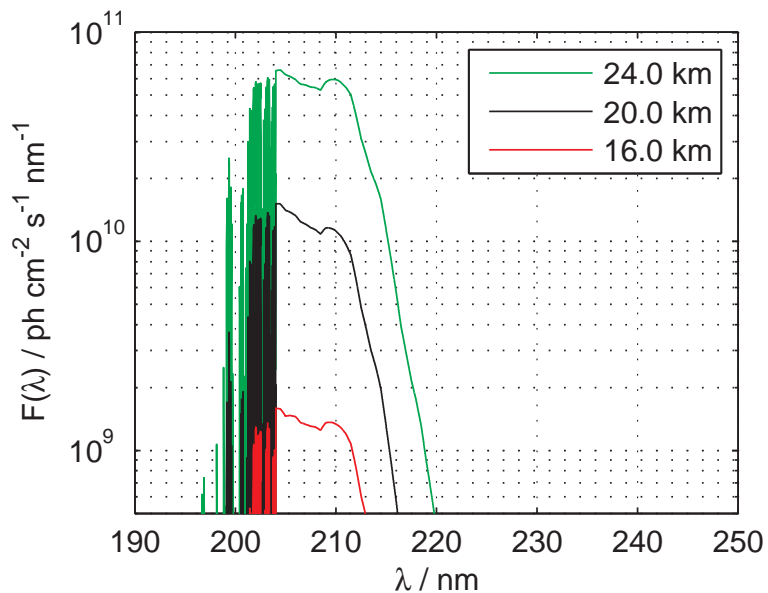


**Fig. 4.** The actinic flux of McLinden et al. (2002) at three different altitudes.

**Isotopic fractionation of stratospheric OCS**

J. A. Schmidt et al.

Title Page

Abstract

Introduction

Conclusions

References

Tables

Figures

◀

▶

◀

▶

Back

Close

Full Screen / Esc

Printer-friendly Version

Interactive Discussion



## Isotopic fractionation of stratospheric OCS

J. A. Schmidt et al.

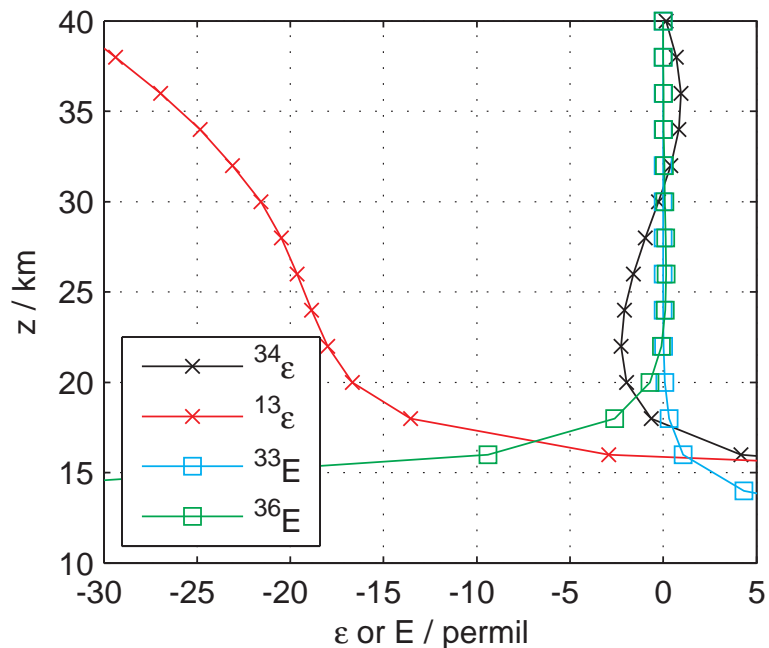


**Fig. 5.** The fractionation constants  $^{34}\epsilon$  and  $^{13}\epsilon$ , and the quantities  $^{33}E$  and  $^{36}E$  as defined in Eqs. (4) and (5) as a function of altitude. The actinic flux as a function of  $z$  was taken from McLinden et al. (2002) while the temperature was modelled using the US standard atmosphere.